Available online at www.sciencedirect.com
ScienceDirect
Physics Procedia 12 (2011) 285–295
Physics Procedia

LiM 2011

Simulation of Light-Propulsion Acceleration of Powder Particles for Laser Direct Metal Deposition

I. O. Kovaleva, O. B. Kovalev*

Khristianovich's Institute of Theoretical and Applied Mechanics, Siberian Branch of Russian Academy of Sciences, Novosibirsk, Russia

Abstract

The results of the numerical analysis of heat- and mass-exchange processes at powder particles motion in a gas flow and radiation during the laser direct metal deposition are presented. The model regarding the particle acceleration due to the light-propulsion force caused by the vapor recoil pressure from the beamed surface of the particle is proposed. The reactive force results in the noticeable particle acceleration toward the radiation direction, and the particle velocity may exceed significantly the velocity of the carrying gas. The radius of particles slightly varies due to the evaporation; the losses in the clad material mass are negligibly small.

Keywords: laser cladding; powder particles; carrying gas; laser radiation; recoil pressure of vapors; light-propulsion force; numerical simulation.

1. Introduction

The processes of laser cladding, direct material deposition (DMD) and rapid prototyping have been studied in a large amount of works; the reviews are presented in a number of monographs [1-3].

C.-Y. Liu et al. [4] studied numerically the process of heating of stainless-steel powder particles by a defocused beam under the conditions approaching to the coaxial laser cladding. To calculate the motion and heating of a single spherical particle in the flow of the carrying gas (argon), they use a known trajectory model which was added by simple particle-size-averaged semiempirical models of melting and heat- and mass-exchange with the ambient gas. The calculations show that the laser heating increases the powder temperature as a whole. At the high power, particles evaporation results in significant powder mass loss, which may reach 25% for steel particles with the diameter of 20 – 200 μm at the radiation power up to 3,000 W.

H. Pan et al. [5] concluded a stochastic model to describe the non-spherical particles collision with the coaxial nozzle wall during the semi-automate laser aided deposition process. The authors can predict correctly the particle flow profile at the nozzle output. However, they concentrate their attention on the flow inside the coaxial nozzle and disregard the problem of particles delivery into the melt pool, where a complex focused jet interaction of the particles, carrying and shaping gas flows takes place on the way between the nozzle and substrate.

* Corresponding author. Tel.: +7-383-330-4273; Fax: +7-383-330-7268.
E-mail address: kovalev@itam.nsc.ru.

doi:10.1016/j.phpro.2011.03.037

The reactive propulsion of the particles in a light field is one among the effects of the interaction between the laser radiation and gas-powder medium. Laser-induced forces can be strong enough to transport small particles in different media. The particles motion in powerful laser-radiation beams has been observed and studied from the sixties of the last century when first lasers occurred. The particle motion can be caused by the light pressure force, reactive and photophoretic forces. The two latter result in turn from the nonuniform heating of particle surface by the laser light [6].

G. A. Askarjan et al. [7, 8] formulated the task of the light-induced reactive acceleration of substance macroparticles with the size of about 1 mm up to 10^5 - 10^6 m/s. Metal crumbs and corundum powder particles were set in the field of ruby laser radiation. It was shown that at the evaporation, the recoil pressure can 3 – 4 orders exceed the light pressure and under normal conditions is the major mechanism of the laser acceleration of the particles.

Waniek R. W. et al. [9] investigated the interaction between the powerful laser radiation with charged particles in order to define the possibility of their acceleration at the expense of the surface evaporation. Aluminum particles of 25 μm in diameter, freely suspended in the time-variant electric field which possessed focusing properties, were located inside a focal spot with the diameter of 100 μm. The spot was generated by a standard ruby laser with the power density of 10^{10} W/m^2 and energy of Joule fractions. Individual laser pulses made their contribution in the stepwise particle acceleration and at the same time provided the stroboscopic monitoring of their trajectories. Due to the recoil pressure at the material evaporation, the velocities of about 200 m/s directed toward the beam action were obtained. The obtained results agree with the momentum conservation law recorded with due regard to the partial particle material evaporation.

Goela J.S. et al. [10] presented the results of the theoretical analysis of the super-powerful laser radiation (above 10^{13} W/m^2) applied for the ablation acceleration of small particles (size from 25 μm to 1 mm) to extremely high speeds (about 10^5 m/s). It was demonstrated that the heating and evaporation nonuniformity makes the particle rotate, which results in speed oscillations perpendicularly to the radiation action. These oscillations may change the particle motion direction and bring it out from the beam region. The authors proposed the method of particle stabilization in the beam owing to the properly chosen intensity density distribution in the beam.

V. I. Bukatyj et al. [11] studied theoretically and experimentally the light-induced propulsion of carbon particles in a laser field. The particles with the size of approximately 100 μm were beamed by the periodical (τ = 1 ms) radiation of a neodymium laser with the wavelength of 1.06 μm and power density in the beam of about 10^8 W/m^2. A single particle was hung of a 50-μm quartz thread. The investigations showed that the maximum particle velocity at the average intensity of the laser radiation of 3.310^8 W/m^2 was 29 m/s. The intensive one-direction expulsion of the heated mass toward the laser beam took place. The observed solid-particle dynamics proved the significant nonuniformity of the particle surface temperature and absence of the mass expulsion in the shadow part of the particle.

The occurring recoil force, caused by the vapor release from the solid body surface, when a laser source was used to produce the jet propulsion, was noted in [12, 13]. Today, there are laser engines based on the evaporation mechanism of the jet propulsion; the propulsion results from the action of the focused radiation on the substance serving as a fuel [13].

In the laser-cladding case, the radiation up to 3 – 5 kW with the focal spot on the substrate of 4 – 6 mm in diameter is normally used, which makes about 10^8 – 10^9 W/m^2 [1-3]. However, the influence of the laser evaporation mechanism on the particles motion in the gas flow at the laser cladding has not been studied yet.

This work is concerned with the study of the powder particles heating and transportation in a gas flow under the conditions of the laser radiation which causes the light-induced acceleration of the particles at the laser cladding.

2. Heat- and mass-exchange of single particles in the gas flow and light field of the laser radiation

Let us consider the conservation laws at the motion of single metal particles in the gas and radiation flow. Let us introduce the force $\vec{F}_R$, which is associated with the particle material evaporation due to the one-sided action of the direct laser radiation on it [12, 13]. If a laser beam falls onto a particle, various evaporation modes may realize on the particle's beamed part. These modes depend on the laser radiation intensity. As the power density in the beam is I_λ, which does not exceed the threshold value, $I_\lambda \le I_{th}$, such a heating mode takes place, when the heat supplied to the particle surface, is able to be released inside the particle owing to thermal-conductivity processes. The particle

heats up, melts, and upon reaching the boiling point of T_{bol} it begins to evaporate intensively. We will call this mode the slow evaporation mode. In the case when the power density in the beam exceeds the threshold value $I_\lambda > I_{th}$, we observe the fast evaporation mode, when the particle surface layer evaporates so fast that the thermal-conductivity processes are not able to participate and the particle is not able even to heat up. In both cases, there is the reaction of material vapors recoil from the beamed particle surface, which results in the reactive force.

Figure 1 show the photo of a focused powder jet produced with the aid of a triple coaxial nozzle (TRUMPF) purposed to organize the flows of shaping and carrying gases and for continuous injection of the powder. General concept of the laser-powder heading is presented schematically in Figure 2. This Figure shows the annular channels of the nozzle, their purpose and the position of the nozzle about the substrate. The peculiarity here is that the powder injection is localized into the laser beam by three coaxially interacting jet flows: the central, or axial one which is intended to protect the optical system; the middle-side one, which transports the powder particles, and the external compressing one, which envelopes the two-phase flow and regulates the size and position of the zone with the maximal particle mass flow.

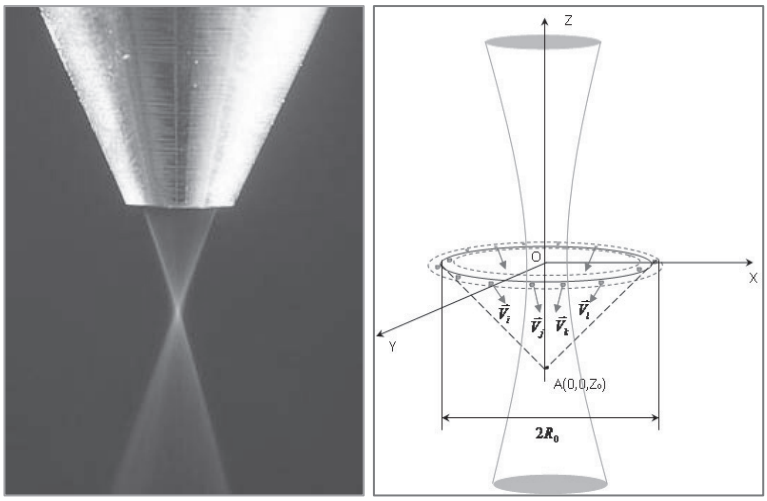

Figure 1, Photo of the laser head (made by TRUMPF) and focused powder jet with the uniformly distributed circular powder injection.
Figure 2, Schematic of the annular powder input, at the initial instant $t = 0$ the particles are located in the plane $z = 0$ near the circle with the radius R_0, velocity vectors directions are focused in the point A.

The cladding process features a melt layer into which powder particles are delivered by the gas jet. The typical size of the particles lies within the range of 20 – 80 μm, the laser beam diameter is 100 – 600 μm. Laser radiation power, focusing, distribution density in the beam and gas flow and particles rates are the governing factors for the cladding.

The assumptions and simplifications used in the physical-mathematical model are the following:

- the 3D task statement in the Cartesian system of coordinates $OXYZ$ is considered;
- the direction of the carrying gas velocity vector $\vec{V}_g = (0,0,w_g)$ coincides with the direction of the beam action and gravity;
- the gas temperature T_g is constant and equal to the initial temperature T_a = 300 K;
- we use the CO_2 laser radiation, its wave length is 10.6 μm, laser-energy power density distribution $I_\lambda(x,y,z)$ is described by the Gaussian function;
- it is assumed that the gas is radiation-transparent, which means that there in no interaction between the gas and laser beam;
- N amount of single spherical particles of the same size with the radius of $r_i \equiv r_0$, $i = 1,2,...,N$ is considered;

- the average by the particle A_i cross section the coefficient of laser radiation absorption K_{ab} is introduced and assumed to be constant;
- particle collisions are absent;
- at the evaporation, owing to the vapor recoil pressure, the light-propulsion force $\vec{F}_{Ri} = (0,0, f_{Ri})$ occurs; its direction coincides with the beam action direction.
- particle rotation is ignored.

For a single spherical particle with the radius r_i, under consideration are the mass center velocity vector $\vec{V}_i = (u_i, v_i, w_i)$ and temperature T_i. The conservation laws for such a particle are written along its trajectory, with due regard to the equation of the variable-mass mechanics [15], the gas flow field is assumed to be predetermined. The motion, heat and mass-exchange equations of an individual particle are written below; they include the predetermined velocity distributions $\vec{V}_g$ and gas temperature T_g, as well as the laser radiation power density distribution $I_\lambda(x, y, z)$.

2.1. The government equations

For the coordinates $\vec{X}_i = (x_i, y_i, z_i)$ and velocities $\vec{V}_i = (u_i, v_i, w_i)$ of the particles, we have the following equations:

$$m_i \frac{d\vec{V}_i}{dt} = \frac{1}{2}\rho_g A_i |\vec{V}_g - \vec{V}_i|(\vec{V}_g - \vec{V}_i)C_{Di} + \vec{F}_{gi} + \vec{F}_{Ri}, \qquad \vec{F}_{gi} = (0,0,g), \tag{1}$$

$$\frac{d\vec{X}_i}{dt} = \vec{V}_i, \qquad \vec{F}_{Ri} = (0,0,f_{Ri}), \quad f_{Ri} = \begin{cases} 0, & T_i < T_m, I_\lambda < I_{th} \\ 0{,}54 A_i P_{vi}, & T_i \geq T_m, I_\lambda < I_{th} \\ A_i I_\lambda K_{ab} u_e / L_e, & I_\lambda \geq I_{th} \end{cases}, \tag{2}$$

where m_i is the mass of the particle; C_{Di} is the drag coefficient; $u_e = \sqrt{0.65\gamma RT_e / M_g}$ is the velocity of material vapor outflow from the particle surface at the evaporation temperature T_e, according to [12] $T_{bol} \leq T_e \leq 1{,}6 \cdot T_{bol}$.

The expression for the light-propulsion force f_{Ri} at the fast evaporation was taken from [13], at the slow evaporation – from [16]. The drag coefficient C_{Di} was calculated by the approximation for the sphere in the non-compressible liquid [17]: $C_{Di} = (24/\mathrm{Re}_i)(1 + 0{,}179\mathrm{Re}_i^{0.5} + 0.013\mathrm{Re}_i)$, $\mathrm{Re}_i < 1000$. Let us write the variation of the full energy of a single particle along its motion trajectory as:

$$\frac{dm_i E_i}{dt} = A_i I_\lambda K_{ab} - H_{gi}(T_i - T_g)S_i - \varepsilon\sigma(T_i^4 - T_g^4)S_i, \tag{3}$$

The right side of the equation (3) regards the heat supply owing to the absorbed laser energy and heat loss for the heat emission and heat exchange with the cold gas flow. The particles temperature is determined with due regard to the heat loss for the melting and evaporation:

$$T_i = \begin{cases} \dfrac{E_i}{C_s}, & E_i \leq C_s T_m \\ T_m, & C_s T_m < E_i \leq C_s T_m + L_f \\ T_{bol}, & C_s T_m + L_f + C_m(T_{bol} - T_m) < E_i \leq C_s T_m + L_f + C_m(T_{bol} - T_m) + L_e \\ T_m + \dfrac{E_i - C_s T_m - L_f - L_e}{C_m}, & E_i \geq C_s T_m + L_f + C_m(T_{bol} - T_m) + L_e \end{cases} \tag{4}$$

To describe the varying particle mass during the evaporation process, the Stefan's law is used [4]:

$$\frac{dm_i}{dt} = -S_i\omega_i\,,\ \omega_i = K_{gi}\frac{M_g}{\gamma R T_g}P_a \ln[\frac{P_a}{P_a - P_{vi}}], \tag{5}$$

Here $E_i = \int_{T_a}^{T_i} C(T_i)dT$ is the specific inner energy of the i-particle at the temperature T_i; P_{vi} is the saturated vapor pressure, according to [4], for steel, $P_{vi} = P_a \exp\left[13.8 - (4.33\times10^4/T_i)\right]$; P_a is the atmospheric pressure. The laser radiation power density $I_\lambda(x,y,z)$ is described by the Gaussian distribution:

$$I_\lambda(x,y,z) = \frac{2W}{\pi\omega_z^2}\exp\left(\frac{2(x^2+y^2)}{\omega_z^2}\right),\ \omega_z^2 = \omega_0^2 + K_\lambda^2\left(z - z_f\right)^2,\ K_\lambda = \frac{\lambda}{\pi\omega_0}. \tag{6}$$

The heat-exchange factor $H_{gi} = Nu\cdot\lambda_g/(2r_i)$ is calculated with the aid of Nusselt: $Nu_i = 2 + 0{,}6(\mathrm{Pr})^{\frac{1}{3}}(\mathrm{Re}_i)^{\frac{1}{2}}$, Prandtl: $\mathrm{Pr} = c_g\mu_g/\lambda_g$, where μ_g, c_g, λ_g is the viscosity, specific heat capacity, gas heat conductivity, and Reynolds numbers: $\mathrm{Re}_i = 2r_i|\vec{V}_g - \vec{V}_i|\rho_g/\mu_g$. The mass-exchange coefficient $K_{gi} = Sh_i\cdot D_g/(2r_i)$ calculation includes the Sherwood: $Sh_i = 2 + 0{,}6(Sc)^{\frac{1}{3}}(\mathrm{Re}_i)^{\frac{1}{2}}$, and Schmidt numbers: $Sc = \mu_g/(D_g\rho_g)$, where D_g is the diffusion coefficient in the gas.

2.2. Method of numerical solution

The initial equations (1 – 7) are transformed and reduced to the system of ordinary differential equations like: $\frac{d\vec{Y}}{dt} = \vec{F}(\vec{Y})$, which is autonomic. Here, the sought vector function is: $\vec{Y} = \{\, x_i,\ y_i\ \ z_i,\ u_i,\ v_i\ \ w_i,\ E_i,\ r_i,$ $i = 1,2,...,N$. For the numerical solution, we used the Runge-Kutta method of the 4th order of accuracy, with the variable time-pitch and automatic control of the assigned calculation accuracy.

2.3. Initial conditions

The annular injection of the powder with the particles jet focused on the beam axis, which is schematically shown in Figure 2, was mathematically simulated as follows. The points on powder injection with the coordinates $x_i(0,x_{i0},y_{i0},0)\equiv x_{i0}$, $y_i(0,x_{i0},y_{i0},0)\equiv y_{i0}$, $z_i(0,x_{i0},y_{i0},0)\equiv 0$ were set uniformly over the circle defined by the equation $x_{i0}^2 + y_{i0}^2 = R_0^2$. The injection points coordinates were defined by the following formulas: $x_{i0} = R_0\sin\left(\frac{2\pi i}{N}\right)$, $y_{i0} = R_0\cos\left(\frac{2\pi i}{N}\right)$. The velocity vector module was pre-determined by the value equal for all particles $\left|\vec{V}_i(0,x_{i0},y_{i0},0)\right| \equiv V_0$, $i = 1,2,...,N$. The direction of the initial velocity vector $\vec{V}_{i0} = (u_{i0},v_{i0},w_{i0})$ of each particle was focused into a certain point A on the beam axis, its coordinates are $A(0,0,z_0)$:

$$u_{i0} = u_i(0,x_{i0},y_{i0},0) = -\frac{V_0 x_{i0}}{\sqrt{x_{i0}^2+y_{i0}^2+z_0^2}},\ v_{i0} = v_i(0,x_{i0},y_{i0},0) = -\frac{V_0 y_{i0}}{\sqrt{x_{i0}^2+y_{i0}^2+z_0^2}},\ w_{i0} = w_i(0,x_{i0},y_{i0},0) = -\frac{V_0 z_0}{\sqrt{x_{i0}^2+y_{i0}^2+z_0^2}}, \tag{7}$$

At the instant $t = 0$, the initial coordinates x_{i0}, y_{i0} and initial particle velocities $\vec{V}_{i0} = (u_{i0},v_{i0},w_{i0})$ were pre-determined with some arbitrary deviations: $x'_{i0} = x_{i0} \pm \delta x_{i0}$, $y'_{i0} = y_{i0} \pm \delta y_{i0}$, $u'_{i0} = u_{i0} \pm \delta u_{i0}$, $v'_{i0} = v_{i0} \pm \delta v_{i0}$, $w'_{i0} = w_{i0} \pm \delta w_{i0}$. The deviations of $\delta x_{i0}, \delta y_{i0}$ and $\delta u_{i0}, \delta v_{i0}, \delta w_{i0}$ were calculated with the aid of a random number

generator. Temperature and particle radius values were pre-determined to be constant at the initial instant: $T_i(0, x_{i0}, y_{i0}, 0) = T_a$, $r_i(0, x_{i0}, y_{i0}, 0) = r_0$.

3. Calculation results

The calculations presented in this chapter are preliminary and their purpose is to show the variation of the powder particle state parameters, namely: velocity, temperature, trajectory and particle diameter with due regard to their localization in the light field of the laser beam. These parameters depend on the radiation characteristics and initial data for the particles and gas. Special attention was paid on the study of the influence of the vapor recoil pressure on the particle motion owing to the mechanism of the one-sided laser evaporation. Thermophysical properties of stainless steel given in Table 1 were used as the data for the particle material.

Table 1. Thermophysical properties of stainless-steel particles

Physical quantity, dimension	Numerical value
Temperature, K: melting T_m /boiling T_{bol}	1809/3137.6
Specific heat, kJ/kg: melting L_f / evaporation L_e	272/6100
Metal density, kg/m^3: solid ρ_s /liquid ρ_m	6900/6610
Specific heat capacity, kJ/(kg K): solid c_s /liquid c_m	0.477/0.810
Radiation absorption coefficient: K_{ab}	0.3
Laser radiation power, W:	500 - 3000
Radiation wave length, μm:	10.6
Gaussian beam radius in the waist, μm: ω_0	300
Lens focus position, mm: z_f	10
Threshold intensity, W/m^2: I_{th}	30 10^8

The typical variation of the particle parameters in the gas flow and radiation flux, when the power varies in the W, as well as when the light-propulsion force ($\vec{F}_{Ri} \equiv 0$) is absent or ($\vec{F}_{Ri} \neq 0$) present is shown in Figure 3, 4, 5. The calculations results are presented in the graph form and grouped in such a way not only to show the particle parameters variation along their trajectories, but also to explain such a behavior. We took 100 particles (N = 100) of the same size and radius r_0 = 45 μm. The defocused Gaussian beam with the waist radius ω_0 = 300 μm and focal plane in the coordinate origin z_f =0 was used. The particle motion was considered within the limits of the divergent beam, $z \le 0$, Figure 2, in the calculation domain $\Omega(x, y, z)$: $x, y \in [-15, +15]$, mm; $z \in [0, -40]$, mm.

3.1. Calculations without the light-propulsion force

The particles begin their motion in the plane z = 0. In the case of $\vec{F}_{Ri} \equiv 0$ their trajectories are almost rectilinear, Figure 3(a). They converge in a certain vicinity of the point ($x = 0$ mm, $z = -17$ mm), then they diverge. As was expected, when the light-propulsion force is ignored ($\vec{F}_{Ri} \equiv 0$), the particle velocities increase monotonically from the injection points $(x_{i0}, y_{i0}, 0), i = 1, 2, ..., N$, with the velocity module $\left|\vec{V}_i(0, x_{i0}, y_{i0}, 0)\right| = (8 \pm 0.8)$ m/s, up to the gas velocity $\left|\vec{V}_g\right|$ = 15 m/s, and this value is still not reached within the whole section under consideration, Figure 3(b).

At the radiation power W = 3,000 W, the particle temperature varies significantly from the initial value T_a = 300 K during a short length (about 15 mm). Some powder particles are able to melt and heat up to the boiling point T_{bol}, Figure 3 (c). The temperature of many particles almost instantly reaches the boiling point. The particles can enter into the light field at certain angles to the OZ axis and leave it freely.

Without the light-propulsion force, the laser radiation does not influence the particles velocity and trajectories. It is also illustrated by the graphs of particle temperature and radius dependence. Figure 3 (d) shows the radius variation because of the evaporation. The temperature of most particles almost instantly reaches the level approaching to the boiling point T_{bol}, the particles begin to evaporate intensively which results in the significant decrease of their diameter (down to 20% from the initial value). It is vital to note that this result agrees with the calculations of the authors of [4], which also ignore the light-induced jet propulsion of the particles.

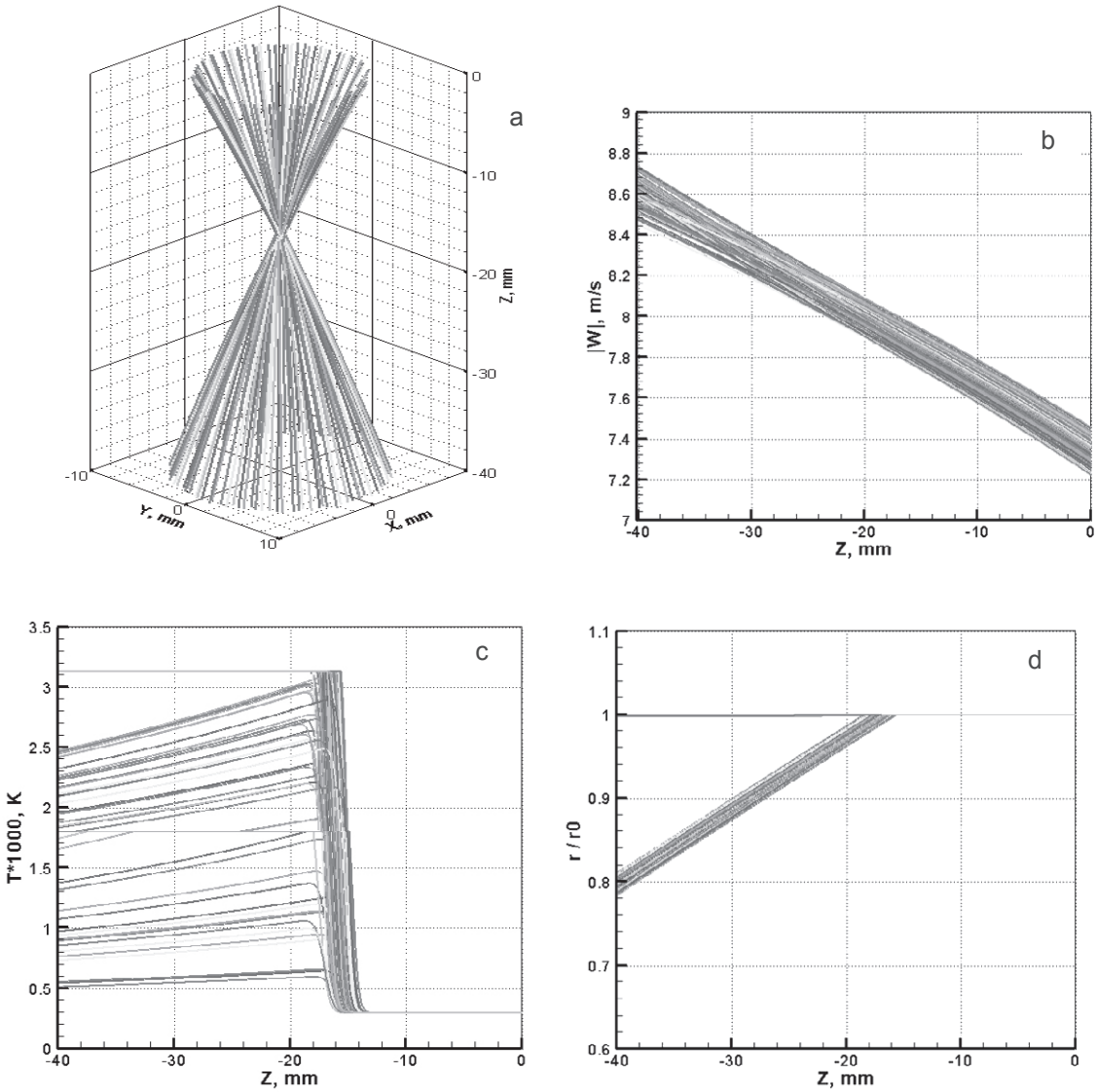

Figure 3, Particles trajectories in the light field of the laser beam (a), particles parameters distribution along the OZ axis: velocity (b); temperature (c); radius (d). The light-propulsion force is missed in the equation (1, 2), $\vec{F}_{Ri} \equiv 0$. Power W = 3,000 W.

Hence, in the case when the radiation power increases, the light-propulsion force being ignored, the particles evaporate intensively. It means that the loss of the deposit material is high. It is not actual for the reality, otherwise the laser cladding effectiveness would have been low. According to the calculations, at $\vec{F}_{Ri} \equiv 0$ the particles trajectories behave in the same way as they do without laser radiation. The calculated shape of the particle flow,

Figure 3(a), rather well agrees with the photo in Figure 1, showing the particle jet is focused by a coaxial nozzle without radiation.

3.2. Calculations with the light-propulsion force

Below it is demonstrated that as the light-propulsion force ($\bar{F}_{Ri} \neq 0$), is included into the momentum conservation law (1, 2), the particles of the powder injected into the flow can get an extra momentum which provides their extra acceleration. In this case, the loss of the particles mass for evaporation is negligibly small.

The varying particles trajectories in the beam region are shown on the background of the Gaussian beam focused in the coordinate origin (Figure 4(a), 5(a)) at the power W of 1,000 and 3,000 W, respectively.

The particles deviate toward the radiation action due to the vapor recoil pressure, their trajectories condense. As the radiation power increases, the condensation intensifies, in practice it enables to localize the powder transport onto the substrate during the cladding process.

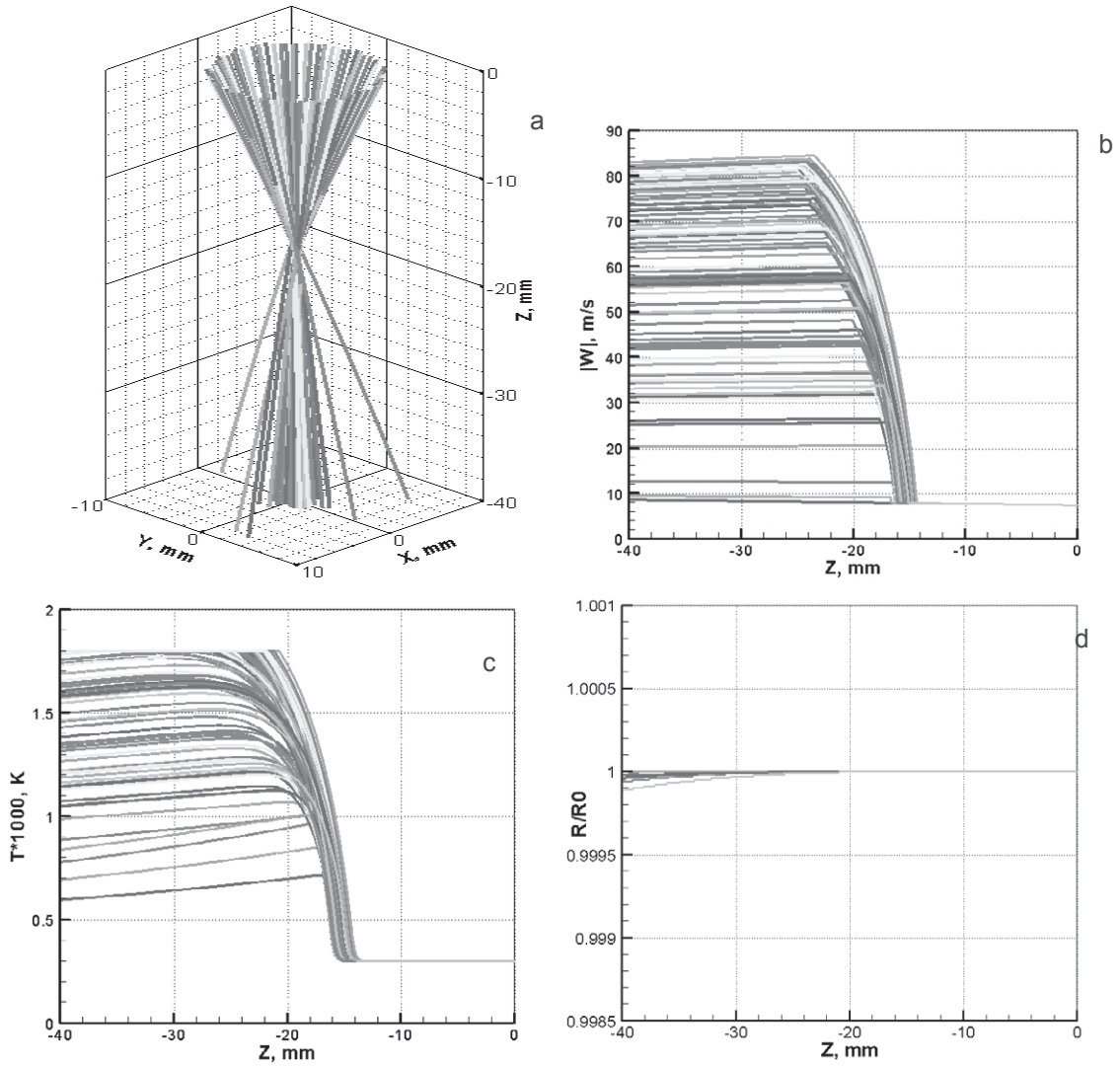

Figure 4, Effect of the light-propulsion force on particle motion trajectories (a) and their parameters: velocity (b); temperature (c); radius (d). Power W = 1,000 W.

The variation of the particle velocities resulting from the light-induced acceleration is of special interest. We observe dramatic increase in the particle velocity when the particle enters into the light field. Figure 4(b), 5(b) show how the velocities of individual particles change along the axis OZ, as the power increases. The velocities of those particles, which trajectories are near the beam axis, increase monotonically from the point of particles entrance in the beam region. Figure 4(b) present the effect of the particles motion with the constant velocity at a certain section where in the mass and light-propulsion and drag forces are balanced. As the power increases, the recoil pressure rises, the particles trajectories remain in the light field and condense even more. Finally, the particles reach the maximum velocity of about 220 m/s at the power of 3,000 W, Figure 5(b).

The thermal state of the particles highly depends on the power density distribution in the beam, on their velocity and motion trajectory in the light field. At W = 1,000 W, the powder particles do not reach the boiling point, not all but few particles are even able to melt, Figure 4(c). The absorbed heat is able, due to the heat conductivity, to be released inside the particle, the particles are heated up and reach the maximum temperature of about 1,200 – 1,800 K. In the case of W = 3,000 W, the particle temperature approaches or reaches the boiling point only at the end of process at z = -40 mm, Figure 5(c). The graphs of the single particles temperature variation have a typical plateau, which occur in the melting and boiling points of the particle material, Figure 5(c). For steel particles, these are T_m = 1800 K and T_{bol} = 3137.6 K. Owing to the light-induced force action, most particles leave the beam region very quickly, they are not even able to heat up properly. Due to the heat exchange with the colder carrying gas, the particle temperature begins to decrease, Figure 5(c).

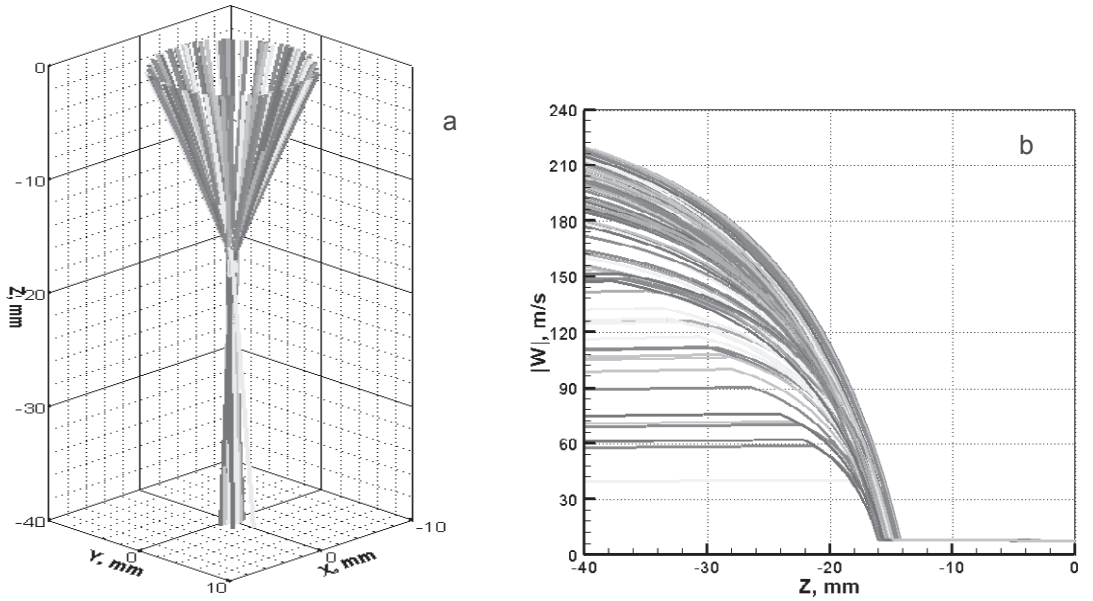

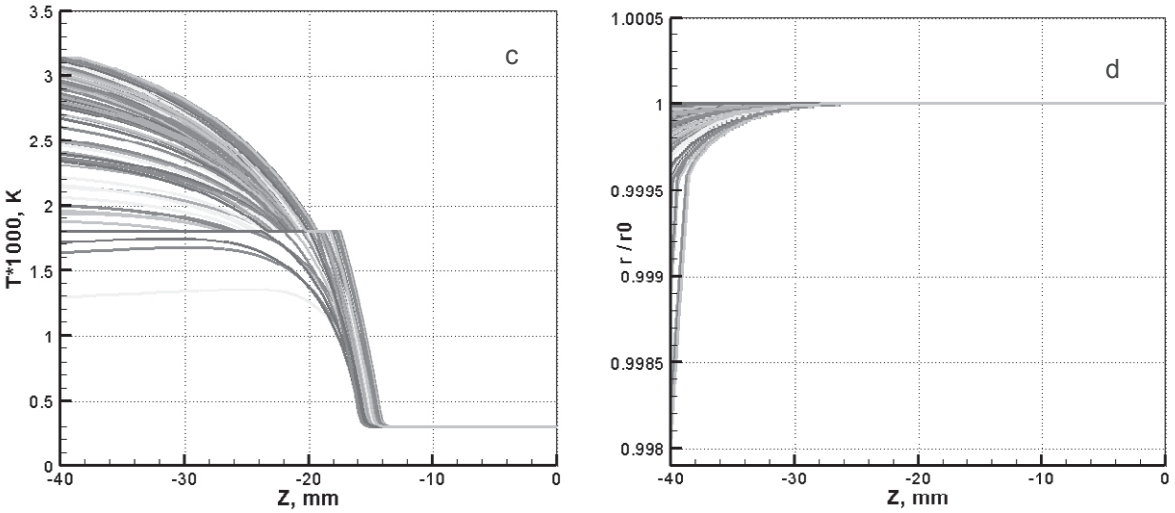

Figure 5, Particles trajectories (a) and their parameters: velocity (b); temperature (c); radius (d). Power W = 3,000 W.

Radiation intensity $I_\lambda(x,y,z)$ decreases with the coordinate z which results in the heat supply decrease. The light-propulsion force does not allow the particles to be heated so that they lose their mass and hence in this case there is almost no variation (below per cent) of the particle diameter, Figure 4(d), 5(d).

4. Conclusions

We propose a model of the heat- and mass-exchange processes when single particles move in the gas flow and light field of the laser radiation in the conditions of the laser cladding and the laser direct metal deposition. The acceleration of the powder particle owing to the force caused by the reaction of the material-vapor recoil from the beamed part of the particle is analyzed and presented.

Performed calculations showed that the light-propulsion force results in the notable acceleration of the particles along with the radiation action, and the particle velocity can be significantly higher than the carrying gas velocity. Due to the recoil pressure, the particles deviate toward the radiation action, their trajectories condense, which enables to localize the powder transport onto the substrate. Particles accelerations depends on their diameter, carrying gas velocity, powder properties, as well as on the laser radiation power, focus degree and beam attenuation toward the action of radiation on the substrate.

Under consideration were the particles of 45 μm in diameter, the radiation power range of the CO_2 laser was 300 – 3,000 W. The particles reach the maximum velocity of about 220 m/s at the power of 3,000. With the light-propulsion force, the particle diameter is almost unchanged, and the mass loss caused by the evaporation is negligibly low.

Acknowledgments

This research was supported by the Russian Foundation for Basic Research (Grant № 08-08-00238_a).

References

[1] Grigorjantz A. G.; Shiganov I. N.; Misyurov A. I.: Technological processes of laser processing. Tutorial for Universities. Moscow: Bauman MGTU. 2007. 664 p. (in Russian)

[2] Lepski D. and Bruckner F.: Laser Cladding. In: J.M. Dowden (ed.). The Theory of Laser Materials Processing (Heat and mass transfer in modern technology). Springer series in material science 119. Springer, Canopus Academic Publishing, 2009.

[3] Panchenko V. Ya.; Golubev V. S; Vasil'tzov V. V. et al.: Laser technologies of materials processing: modern challenges of fundamental researches and applied developments. Moscow: Fizmatlit, 2009. 664 p. (in Russian)

[4] Liu Chang-Yi and Lin J.: Thermal processes of a powder particle in coaxial laser cladding// Optics and Laser Technology. 2003. Vol. 35, pp. 81-86.

[5] H. Pan and F. Liou, Numerical Simulation of Metallic Powder Flow in a Coaxial Nozzle for the Laser Aided Deposition Process, *Journal of Materials Processing Technology*, 2005, Vol. 168, p 230-244

[6] Ashkin A.: The Pressure of Laser Light, Scientific American **226** (2), 63 (1972).

[7] Askarjan G. A.; Moroz E. M.: The pressure at the substance evaporation in the radiation beam // ZhETF (Journal of Experimental and Theoretical Physics). 1962. Vol. 43, Issue 6. Pp. 2319-2320. (in Russian)

[8] Askarjan G. A.; Rabinovich M. S.; Savchenko M. M. et al.: Light-induced acceleration of substance macroparticles // Letters of ZhETF (Journal of Experimental and Theoretical Physics). 1967. Vol. 5, Issue 8. Pp. 258-260. (in Russian)

[9] Waniek R. W. and Jarmuz P. J.: Acceleration of Microparticles by Laser-induced Vapor Emission // Applied Physics Letters. 1968.Vol. 12, No. 2. P. 52-54.

[10] Goela J. S. and Green B. D.: Ablative acceleration of small particles to high velocity by focused laser radiation // J. Opt. Soc. Am. B. 1986. Vol. 3, No. 1, pp. 8-14.

[11] Bukatyj V. I.; Kronberg T. K.: Light-induced propulsion of a carbon particle in the powerful laser field // Izvestia Altajskogo Gosudarstvennogo Universiteta. 1996. Vol. 1(1). Pp. 50-53. (in Russian).

[12] Bunkin F. V.; Prokhorov A. M.: Laser energy source used for reactive drag generation // Success in Physics. 1976. Vol. 119, Issue 3. Pp. 425-446. (in Russian).

[13] Prokhorov A. M.; Konov V. I.; Ursu I. et al.: Interaction between laser radiation and metals. Moscow: Nauka, 1988. 537 p. (in Russian)

[14] Volkov K. V.; Emel'janov V. N.: Flow of the gas with particles. Moscow: Fizmatlit, 2008. 600 p. (in Russian)

[15] Mescherskij I. V.: Works on the mechanics of variable-mass bodies, 2nd issue, Moscow, 1952; (in Russian)

[16] Anisimov S. I.; Imas Ya. A.; Romanov G. S., Khodyko Yu. V.: The action of high-power radiation on metals. Moscow: Nauka, 1970. (in Russian).

[17] Gavin L.B. and Naumov V.A.: Turbulent two-phase jet and its numerical investigation // Journal of Engineering Physics and Thermophysics. 1983. Vol. 44, No. 6, pp. 623-628.